

# Electrochemical performance and spectroscopic characterization of TiO<sub>2</sub>-coated LiNi<sub>0.8</sub>Co<sub>0.2</sub>O<sub>2</sub> cathode materials

Z.R. Zhang, H.S. Liu, Z.L. Gong, Y. Yang\*

State Key Laboratory for Physical Chemistry of Solid Surfaces, Department of Chemistry, Xiamen University, Xiamen 361005, PR China

## Abstract

Electrochemical performance and spectroscopic characterization of native and TiO<sub>2</sub>-coated LiNi<sub>0.8</sub>Co<sub>0.2</sub>O<sub>2</sub> were investigated. The electrochemical results showed TiO<sub>2</sub>-coated materials exhibited better cycle stability in the different potential regions (i.e. 3.0–4.3 and 3.0–4.6 V) and the decomposition of the electrolytes was suppressed on coated materials surface. In addition, FT-IR and temperature-programmed desorption–mass spectroscopy (TPD–MS) results demonstrated that different oxidation products were formed on the native and coated electrodes. A possible decomposition mechanism of the electrolytes has been proposed based on our results.

© 2003 Elsevier B.V. All rights reserved.

**Keywords:** LiNi<sub>0.8</sub>Co<sub>0.2</sub>O<sub>2</sub>; Titanium dioxide; Surface coating; Lithium ion batteries

## 1. Introduction

LiNi<sub>0.8</sub>Co<sub>0.2</sub>O<sub>2</sub> is a very promising cathode material with high capacity and medium cost for lithium ion secondary cells [1]. It is a competent substitute for commercialized LiCoO<sub>2</sub>, after its cycle performance and thermal stability are further improved. Many studies have suggested surface coating is a useful way for improving the properties of LiNi<sub>0.8</sub>Co<sub>0.2</sub>O<sub>2</sub> [2–7]. However, the mechanism of improved cycling performance affected by the surface coating is still not clear.

In order to understand improved performance of the coated materials properly, the detection of the reaction products formed after electrochemical reactions on the coated materials is necessary through the help of different spectroscopic techniques. FT-IR is a powerful technique to characterize the absorbed species on the material surface, and temperature-programmed desorption–mass spectroscopy (TPD–MS) can be applied to obtain the mass–electric charge ratio ( $m/e$ ) of the species adsorbed on material surface. The combination of the two techniques should confidently determine species adsorbed on the electrode surface, which is helpful to understand the decomposition mechanism of the electrolytes.

In this work, TiO<sub>2</sub>-coated LiNi<sub>0.8</sub>Co<sub>0.2</sub>O<sub>2</sub> materials were synthesized by a sol–gel method and their electrochemical performance were investigated. FT-IR and TPD–MS techniques are applied to investigate the decomposition products

of the electrolyte on the cathode material surface. The oxidation mechanisms of the electrolytes on electrodes surface are proposed based on our spectroscopic results.

## 2. Experimental

LiNi<sub>0.8</sub>Co<sub>0.2</sub>O<sub>2</sub> powders were synthesized by sol–gel method using citric acid as chelating agent, which has been reported in our previous work [8]. The TiO<sub>2</sub>-coated LiNi<sub>0.8</sub>Co<sub>0.2</sub>O<sub>2</sub> powders were synthesized by the hydroxylation of tetra-*n*-butyl titanate (TBT) in air and the mole ratio of Ti: LiNi<sub>0.8</sub>Co<sub>0.2</sub>O<sub>2</sub> is 0.03. The sintering condition was controlled at 400 °C for 5 h in air. The thickness of the coating layer was about 20–35 nm by means of SEM and TEM image [9].

Cavity powder microelectrodes (CME) were made of a glass tube containing a Pt-wire (diameter: 100 μm) inside [9]. The usual height–diameter of the cavity ratio was between 0.4 and 0.8.

The electrochemical experiments of the powder microelectrodes were performed using a CHI 600 A Potentiostat/Galvanostat System (Shanghai, China). A Li foil pressed into Ni net was served as the counter and reference electrodes. The electrolyte was 1 M LiPF<sub>6</sub>/EC+DMC (1:1). The potential scan rate was 10 mV/s in the cyclic voltammety (CV) experiment. The ac perturbation signal was ±5 mV and the frequency range was from 1 to 10<sup>4</sup> Hz in the impedance experiments. The electrochemical cycling stabilities of the materials were assessed using CR2025 coin cells. The cathodes were prepared by mixing 85% of the active material

\* Corresponding author. Tel./fax: +86-592-2185753.

E-mail address: [yyang@xmu.edu.cn](mailto:yyang@xmu.edu.cn) (Y. Yang).

with 10% carbon black and 5% PVDF. The cells were assembled with the cathode as prepared, lithium metal as anode, and Celgard 2300 film as separator. Cell assembling was carried out in an argon-filled glove box (Mode 100G, M. Braun, Germany,  $\text{H}_2\text{O} < 5 \text{ ppm}$ ). Charge–discharge experiments were performed with  $0.2 \text{ C}$  ( $\sim 36 \text{ mA/g}$ ) current in different potential region using an Arbin Battery Cycler (USA).

All FT-IR measurements of electrodes were carried out by using a micro-IR spectrometer (Nicolet AVATAR 360 + Centaur $\mu\text{s}$  IR Microscope, USA). The electrodes after cycling were washed immediately with pure ethanol for several times and dried under infrared light for 10 min. The spectral resolution was set at  $2 \text{ cm}^{-1}$  and all spectra were collected by 128 scans in the IR experiments.

Temperature-programmed desorption–mass spectroscopy (TPD–MS) experiments were performed by Qminstar QMS

200 (USA). Firstly, the cathode materials were pressed directly on Al foil, the 300 cycles CV experiments were performed, then the electrodes were disassembled in glove box and were placed in the box for 24 h to evaporate the liquid electrolyte. Finally, the powders were scraped from the Al foil and used for the TPD–MS experiments. Helium (He) served as loading gas, the collection time of each channel was 0.5 s and the rate of increasing temperature was controlled at  $15^\circ\text{C}/\text{min}$ .

### 3. Results and discussion

#### 3.1. Electrochemical behavior

Fig. 1 shows multi-cyclic voltammograms of uncoated and  $\text{TiO}_2$ -coated  $\text{LiNi}_{0.8}\text{Co}_{0.2}\text{O}_2$  materials in different

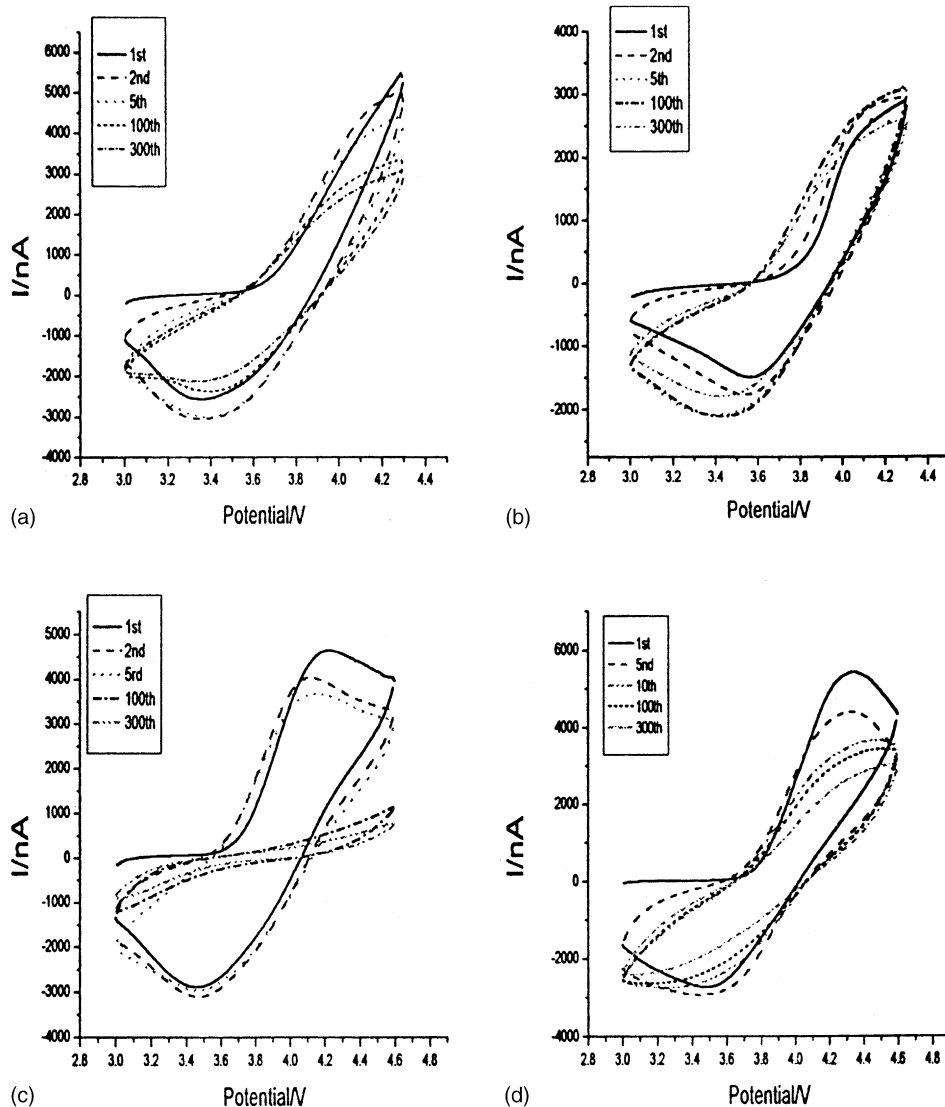


Fig. 1. Cyclic voltammograms of  $\text{LiNi}_{0.8}\text{Co}_{0.2}\text{O}_2$  with and without  $\text{TiO}_2$  coating at  $10 \text{ mV/s}$  in  $1 \text{ M LiPF}_6/\text{EC} + \text{DMC}$  (1:1) in different potential regions: (a) uncoated  $\text{LiNi}_{0.8}\text{Co}_{0.2}\text{O}_2$ ,  $3.0\text{--}4.3 \text{ V}$ ; (b)  $\text{TiO}_2$ -coated  $\text{LiNi}_{0.8}\text{Co}_{0.2}\text{O}_2$ ,  $3.0\text{--}4.3 \text{ V}$ ; (c) uncoated  $\text{LiNi}_{0.8}\text{Co}_{0.2}\text{O}_2$ ,  $3.0\text{--}4.6 \text{ V}$ ; (d)  $\text{TiO}_2$ -coated  $\text{LiNi}_{0.8}\text{Co}_{0.2}\text{O}_2$ ,  $3.0\text{--}4.6 \text{ V}$ .

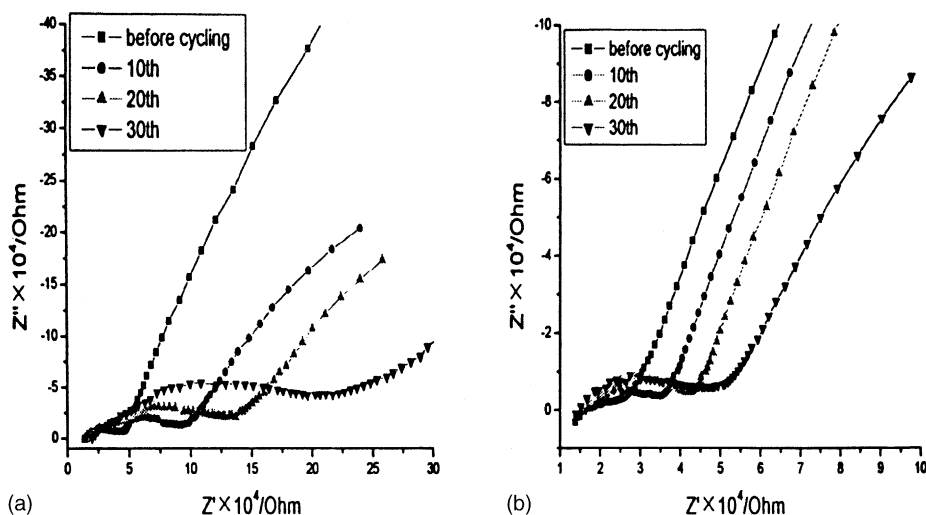


Fig. 2. The ac impedance spectra of the uncoated (a) and  $\text{TiO}_2$ -coated (b)  $\text{LiNi}_{0.8}\text{Co}_{0.2}\text{O}_2$  before and after multiple cycling at 10 mV/s in 3–4.6 V in 1 M  $\text{LiPF}_6/\text{EC} + \text{DMC}$  (1:1).

potential regions at the rate of 10 mV/s. The coated electrodes exhibit good cycle stability no matter that the upper cutoff potential is 4.3 or 4.6 V as shown in Fig. 1(b) and (d), respectively. In comparison, the uncoated  $\text{LiNi}_{0.8}\text{Co}_{0.2}\text{O}_2$  shows a poor cyclic stability during cycling as shown in Fig. 1(a) and (c). The latter, where the electrode was cycled in 3–4.6 V, the stability of the material is very poor. After 300 repeat cyclings, the electrochemical activity decreased dramatically as shown in Fig. 1(c). This may imply that the charge transfer resistance of the electrodes has greatly increased.

Fig. 2 compares the EIS profiles of the bare and  $\text{TiO}_2$ -coated  $\text{LiNi}_{0.8}\text{Co}_{0.2}\text{O}_2$  before and after cycling at 10 mV/s in the 3–4.6 V region. All the EIS profiles in Fig. 2 consist of a high and a low frequency arc. In general, the low frequency arc contains the contribution of the contact impedance between inter-particles, while the high frequency arc can be attributed to the charge transfer process in the electrode/electrolyte interface; namely, the change of the high frequency arc size may reflect the growth of a passive surface film formed by the reaction between the lithiated metal oxide and electrolytes [10,11]. As shown in Fig. 2, the size of the high frequency arc of the uncoated material increases more sharply than that of the coated material. This can be interpreted as the formation of surface film is restrained and the decomposition reaction of the electrolytes is suppressed on the coated  $\text{LiNi}_{0.8}\text{Co}_{0.2}\text{O}_2$  surface with  $\text{TiO}_2$ . This is further confirmed in the following FT-IR experiments.

Fig. 3 compares the cycling stability of uncoated and  $\text{TiO}_2$ -coated  $\text{LiNi}_{0.8}\text{Co}_{0.2}\text{O}_2$  cathodes in the voltage ranges of 3.0–4.3 and 3.0–4.6 with 0.2 C ( $\sim 36$  mA/g) current at room temperature. Despite less initial discharge capacity, the coated material shows better cycling stability than pristine material in various voltage ranges. The specific discharge capacity of pristine material decreases to 113 mAh/g

after 100 cycles with retention of 65% for 4.3 V, while that of coated material only changes to 140 mAh/g at the 100th cycle with retention of 84%. When the cutoff charge potential was 4.6 V, the initial discharge specific capacity of pristine material increased to 205 mAh/g but only retained 51% after 100 cycles, while that of coated material even keeps 158 mAh/g at the 100th cycle with retention of 80%. It is noted that the pristine material exhibits serious capacity fade in earlier cycles for 4.6 V, which may be attributed to different properties of passive surface film. Our other experimental results have indicated  $\text{TiO}_2$ -coated material cannot suppress phase transitions as Ti-doped material [12], which means that the improved cycling stability of coated material is not originated from the suppression of phase transitions. It should be noted that the capacity fading of lithium nickel oxides is a complex phenomenon which is related to both bulk structure and interface instability. Based on our above results, the positive effect of coated material should be attributed to the enhanced interface stability.

### 3.2. FT-IR

The Fourier transform infrared reflection (FT-IR) spectra of the coated and uncoated  $\text{LiNi}_{0.8}\text{Co}_{0.2}\text{O}_2$  particles in the microcavity before and after 300 cycles in different potential regions are shown in Fig. 4. A new band at about  $1510\text{ cm}^{-1}$  is assigned to the  $\text{RCO}_2^-$  stretching vibration [13,14]. This band must come from the decomposition products of EC and/or DMC. Therefore, it is concluded that the decomposition products of electrolytes in these electrochemical experiments are mainly carboxylate salts  $\text{RCO}_2^-$ . In addition, as seen in Fig. 4, the intensity of this band for the coated electrode is weaker than that for the uncoated electrode and it hardly increases in the higher potential cycling. These results indicate that the decomposition of electrolytes on the

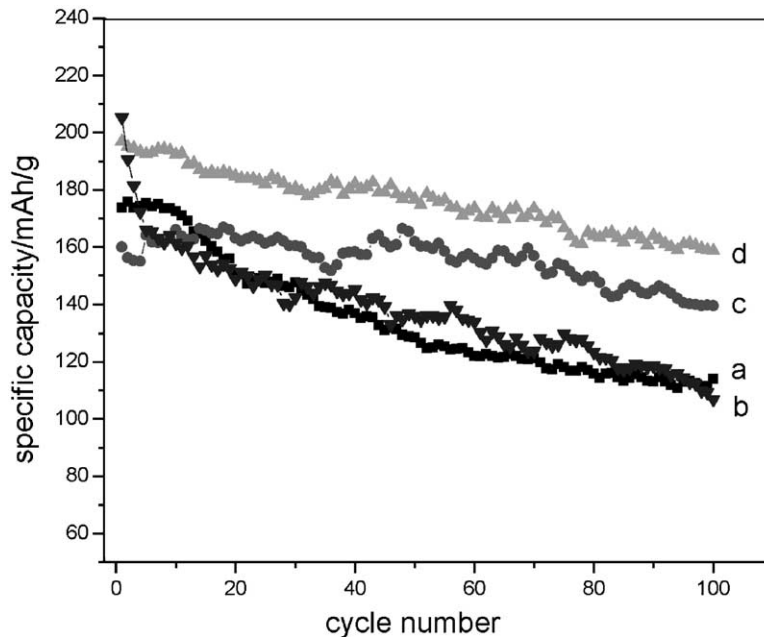


Fig. 3. Comparison of the cycling stability of uncoated and  $\text{TiO}_2$ -coated  $\text{LiNi}_{0.8}\text{Co}_{0.2}\text{O}_2$  cathodes in different voltage ranges at  $C/5$  rate in 1M  $\text{LiPF}_6/\text{EC} + \text{DMC}$  (1:1): (a) uncoated  $\text{LiNi}_{0.8}\text{Co}_{0.2}\text{O}_2$  (3.0–4.3 V); (b) uncoated  $\text{LiNi}_{0.8}\text{Co}_{0.2}\text{O}_2$  (3.0–4.6 V); (c)  $\text{TiO}_2$ -coated  $\text{LiNi}_{0.8}\text{Co}_{0.2}\text{O}_2$  (3.0–4.3 V); (d)  $\text{TiO}_2$ -coated  $\text{LiNi}_{0.8}\text{Co}_{0.2}\text{O}_2$  (3.0–4.6 V).

coated electrode surface is much weaker, leading to less decomposition products. It is concluded that the decomposition of organic electrolytes at high potential is suppressed when  $\text{TiO}_2$  is coated on the  $\text{LiNi}_{0.8}\text{Co}_{0.2}\text{O}_2$  particles surface. This is in good agreement with the EIS results.

The suppressed decomposition of the electrolyte on the coated materials is readily understood in terms of a  $\text{Ni}^{4+}$  intermediacy which is well known to have very strong oxida-

tion ability. At a high potential,  $\text{Ni}^{4+}$  is formed significantly on a bare, highly deintercalated state  $\text{Li}_x\text{Ni}_{0.8}\text{Co}_{0.2}\text{O}_2$  surface and these  $\text{Ni}^{4+}$  must oxidize the electrolyte. In contrast,  $\text{Ti}^{4+}$  is a very stable ion without high oxidation capability. When the cathode particle surface was coated with  $\text{TiO}_2$ , its bulk materials which contained  $\text{Ni}^{4+}$  were isolated from the electrolytes. Therefore, the oxidation processes of the electrolytes are suppressed.

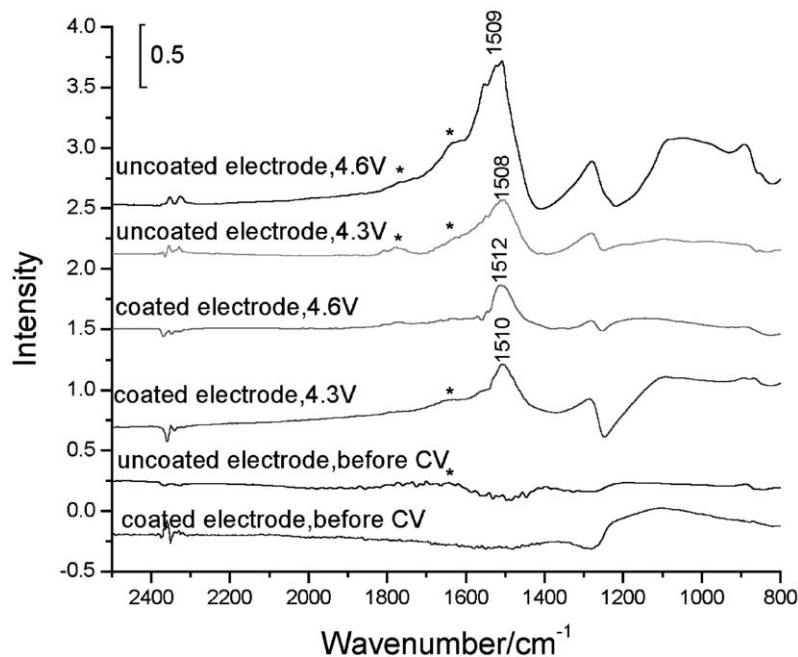
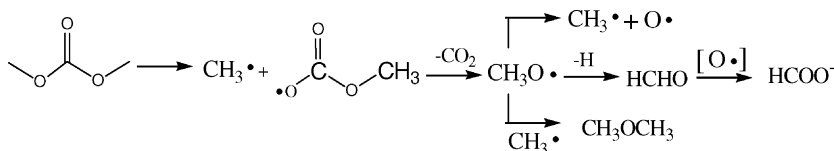


Fig. 4. FT-IR spectra of the uncoated and  $\text{TiO}_2$ -coated  $\text{LiNi}_{0.8}\text{Co}_{0.2}\text{O}_2$  before and after 300 cyclings in 1M  $\text{LiPF}_6/\text{EC} + \text{DMC}$  (1:1) (\* peaks may represent the residual electrolyte). The experimental conditions of the samples have been labeled above each spectrum.

### 3.3. TPD-MS

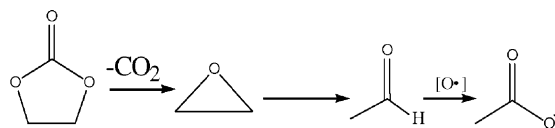
In order to investigate in depth these decomposition products, a series of TPD-MS experiments were performed. With the increase of the temperature, the species of  $m/e$  20, 30, 32, 44, 45, 46, 69, 85, 104 and 88 were simultaneously observed for both electrode materials. The assignments of possible structure for these species are shown in Table 1. It is noteworthy that whereas the species of  $m/e$  59, 73, 87 that correspond to  $\text{CH}_3\text{COO}^-$ ,  $\text{CH}_3\text{CH}_2\text{COO}^-$  and  $\text{C}_3\text{H}_7\text{COO}^-$  (Table 1) are observed for the uncoated electrode materials (Fig. 5), respectively, only the last species of  $m/e$  87 was observed for the  $\text{TiO}_2$ -coated electrode material. The disparity observed in TPD-MS experiments indicates a dissimilarity in electrolyte decomposition routes.

The TPD-MS experiments of the two electrode materials before and after 300 cycles in pure DMC as the electrolyte between 3 and 4.6 V were also performed. The results showed that the species of  $m/e$  30, 45 and 46 could be observed only after cycling, that is, the decomposition products of DMC are  $\text{HCHO}$ ,  $\text{HCOO}^-$ , etc. that are generated through an electrochemical process as depicted below.



For the small amount of  $\text{CH}_3\text{CO}_2^-$  generated in  $\text{LiPF}_6/\text{EC} + \text{DMC}$  electrolytes on the uncoated electrode surface (Fig. 5c), it is most reasonable to propose EC is the source, and in analogy to the suggestion by Arakawa and Yamaki [15], follows the following mechanism involving a

1,2-proton shift:



Because of the effect of electric fields, the electron cloud on the carboxyl ( $-\text{COO}^-$ ) is attracted by the positively charged electrode surface. Therefore the  $\beta$ -C of  $\text{CH}_3\text{COO}^-$  is electropositive due to the induction effect, it is easily attacked by  $\text{CH}_3\cdot$  and generates  $\text{CH}_3\text{CH}_2\text{COO}^-$ ,  $(\text{CH}_3)_2\text{CHCOO}^-$ . However,  $(\text{CH}_3)_2\text{CHCOO}^-$  is very difficult to react further with  $\text{CH}_3\cdot$  due to the effect of space. Consequently, the amount of  $(\text{CH}_3)_3\text{CCOO}^-$  is negligible or too little to observe in the TPD-MS experiment. The reaction route may be expressed in the following path:

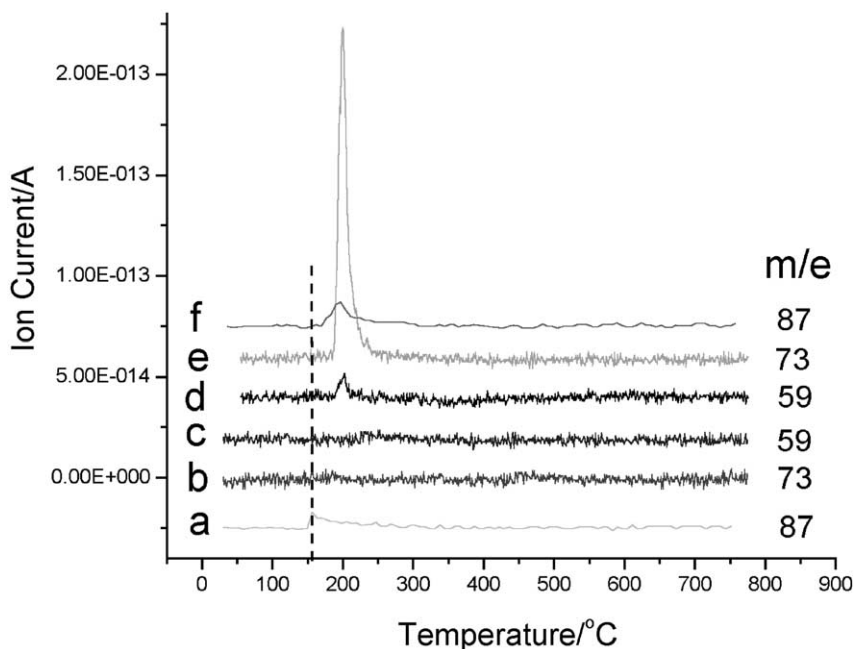
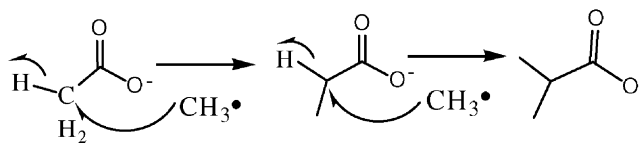


Fig. 5. TPD-MS results of the  $\text{TiO}_2$ -coated (a, b, c) and uncoated  $\text{LiNi}_{0.8}\text{Co}_{0.2}\text{O}_2$  (d, e, f) after 300 cycles in 1 M  $\text{LiPF}_6/\text{EC} + \text{DMC}$  (1:1) in the 3–4.6 V scan potentials range.

Table 1

The mass/electron ratio ( $m/e$ ) and corresponding assignment of the decomposition products on coated and uncoated electrode surfaces

$m/e$	Assignment	Uncoated electrode	Coated electrode
20	HF	+ <sup>a</sup>	+
30	HCHO	+	+
32	O <sub>2</sub> or CH <sub>3</sub> OH	+	+
44	CO <sub>2</sub> or CH <sub>3</sub> CHO	+	+
45	HCOO <sup>-</sup>	+	+
46	CH <sub>3</sub> OCH <sub>3</sub>	+	+
59	CH <sub>3</sub> COO <sup>-</sup>	+	- <sup>b</sup>
69	PF <sub>2</sub>	+	+
73	C <sub>2</sub> H <sub>5</sub> COO <sup>-</sup>	+	-
85	POF <sub>2</sub>	+	+
87	C <sub>3</sub> H <sub>7</sub> COO <sup>-</sup>	+	+
88	EC	+	+
104	POF <sub>3</sub>	+	+

<sup>a</sup> + represents the presence of the species.

<sup>b</sup> - represents the absence of the species.

is firstly partially absorbed on the electrode surface and those excessive and free CH<sub>3</sub>COO<sup>-</sup> can react with CH<sub>3</sub>• to generate CH<sub>3</sub>CH<sub>2</sub>COO<sup>-</sup>. Similarly, CH<sub>3</sub>CH<sub>2</sub>COO<sup>-</sup> is also absorbed on the electrode surface after its formation. Therefore, CH<sub>3</sub>COO<sup>-</sup> and CH<sub>3</sub>CH<sub>2</sub>COO<sup>-</sup> can be detected in the TPD-MS experiment of the uncoated electrode. However, for the coated electrode, the interaction between carboxylate ion and TiO<sub>2</sub> is much weaker and carboxylate anions cannot be adsorbed well on the coated electrode surface. These newly formed carboxyl salts on the coated electrodes should react continuously with CH<sub>3</sub>• and yield (CH<sub>3</sub>)<sub>2</sub>CHCOO<sup>-</sup>. Further research of the electrolyte decomposition mechanism is in progress in the laboratory.

#### 4. Conclusion

The electrochemical and FT-IR experiments indicated TiO<sub>2</sub>-coated electrodes showed better cyclic performance, the enhanced cycling stability may be attributed to the suppression of the electrolytes decomposition on coated materials surface. In addition, the TPD-MS experiments indicated that the electrolyte decomposition

products on the two materials surface were different. Besides POF<sub>x</sub><sup>-</sup> salt, the electrolyte decomposition products on the coated LiNi<sub>0.8</sub>Co<sub>0.2</sub>O<sub>2</sub> surface mainly were HCOO<sup>-</sup>, (CH<sub>3</sub>)<sub>2</sub>CHCOO<sup>-</sup>, whereas the products on the uncoated electrode surface included HCOO<sup>-</sup>, CH<sub>3</sub>COO<sup>-</sup>, CH<sub>3</sub>CH<sub>2</sub>COO<sup>-</sup> and (CH<sub>3</sub>)<sub>2</sub>CHCOO<sup>-</sup>. The difference of the electrolyte decomposition mechanisms may be caused by the interaction between carboxyl salts and the electrode surface.

#### Acknowledgements

This work was financial supported by the National Natural Science Foundation of China (No. 20021002, 29925310, 29833090).

#### References

- [1] C. Delmas, M. Menetrier, L. Croguennec, et al., *Electrochim. Acta* 45 (1999) 243.
- [2] J. Cho, T.J. Kim, Y.J. Kim, et al., *Electrochem. Solid State Lett.* 4 (2001) A159.
- [3] B.V.R. Chowdari, G.V.S. Rao, S.Y. Chow, *J. Solid State Electrochem.* 6 (2002) 565.
- [4] Z.H. Chen, J.R. Dahn, *Electrochem. Solid State Lett.* 5 (2002) A213.
- [5] J. Cho, C.S. Kim, S.I. Yoo, *Electrochem. Solid State Lett.* 3 (2000) 362.
- [6] J. Cho, Y.J. Kim, B. Park, *Chem. Mater.* 12 (2000) 3788.
- [7] A.M. Kannan, L. Rabenberg, A. Manthiram, *Electrochem. Solid State Lett.* 5 (2002) A213.
- [8] H.S. Liu, J. Li, Z.R. Zhang, et al., *J. Solid State Electrochem.* 7 (2003) 456–462.
- [9] Z.R. Zhang, H.S. Liu, Z.L. Gong, et al., *J. Electrochem. Soc.*, in press.
- [10] M.D. Levi, G. Salitra, B. Markovsky, et al., *J. Electrochem. Soc.* 146 (2002) 1279.
- [11] K.A. Striebel, E. Sakai, E.J. Cairns, *J. Electrochem. Soc.* 149 (2002) A61.
- [12] H.S. Liu, Z.R. Zhang, Z.L. Gong, et al., *Solid State Ionics*, in press.
- [13] K. Kanamura, *J. Power Sour.* 81–82 (1999) 123.
- [14] F. Joho, P. Novak, *Electrochim. Acta* 45 (2000) 3589.
- [15] M. Arakawa, J. Yamaki, *J. Power Sour.* 54 (1995) 250.